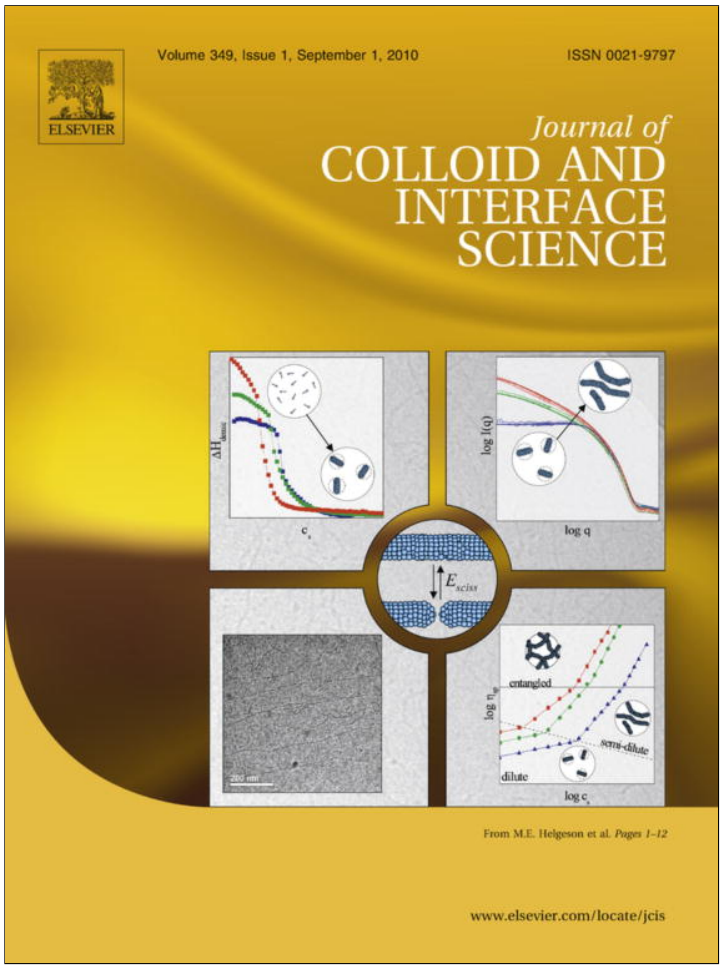

Journal of Colloid and Interface Science 349 (2010) 283–292

Contents lists available at ScienceDirect

Journal of Colloid and Interface Science

www.elsevier.com/locate/jcis

Adsorption and corrosion-inhibiting effect of *Dacryodis edulis* extract on low-carbon-steel corrosion in acidic media

E.E. Oguzie *, C.K. Enenebeaku, C.O. Akalezi, S.C. Okoro, A.A. Ayuk, E.N. Ejike

Electrochemistry and Materials Science Research Laboratory, Department of Chemistry, Federal University of Technology Owerri, PMB 1526, Owerri, Nigeria

ARTICLE INFO

Article history:
Received 12 March 2010
Accepted 11 May 2010
Available online 15 May 2010

Keywords:
Steel
Acid corrosion
Plant extracts
Molecular modeling
Adsorption

ABSTRACT

The inhibition of low-carbon-steel corrosion in 1 M HCl and 0.5 M H_2SO_4 by extracts of *Dacryodis edulis* (DE) was investigated using gravimetric and electrochemical techniques. DE extract was found to inhibit the uniform and localized corrosion of carbon steel in the acidic media, affecting both the cathodic and anodic partial reactions. The corrosion process was inhibited by adsorption of the extracted organic matter onto the steel surface in a concentration-dependent manner and involved both protonated and molecular species. Molecular dynamics simulations were performed to illustrate the process of adsorption of some specific components of the extract.

1. Introduction

Iron and its alloys find extensive structural applications in industry and engineering construction, where they are used in a variety of service environments. The aggressive nature of some service environments often leads to excessive corrosion of exposed metal surfaces, which is a major cause for concern. A significant method for protecting such metals is the introduction of corrosion inhibitors that hinder the corrosion reaction and thus reduce the corrosion rate. Owing to increasing ecological awareness and strict environmental regulations, as well as the inevitable drive toward sustainable and environmentally friendly processes, attention is now focused on the development of nontoxic alternatives to inorganic and organic inhibitors applied earlier. Consequently, the current focus in corrosion inhibitor research is on identifying and developing new classes of nontoxic, benign, and inexpensive alternatives. In this regard, there has been increasing interest in investigating natural products of plant origin for corrosion-inhibiting efficacy [1–10]. Such studies are justified by the phytochemical compounds present therein, with molecular and electronic structures bearing close similarity to those of conventional organic inhibitor molecules. In addition, plant products are low-cost, readily available, and renewable sources of materials.

Despite the high availability and many varieties of plant materials, only relatively few have been thoroughly investigated, and even at that, reports on the detailed mechanisms of the adsorption process are still scarce. The present report continues to focus on the broadening application of plant extracts for metallic corrosion control and reports on the inhibiting effect of leaf extracts of *Dacryodis edulis* (DE) on low-carbon-steel corrosion in acidic solutions. Ascorbic acid (AA) has been identified as the major chemical constituent of the plant and an alkaloid, 2-[2H-1,2,3-benzotriazo-2-yl)-4-methylphenyl-3-benzoate (HBMB; $C_{21}H_{17}N_3O_2$), has also been isolated [11]. β-Caryophyllene (Cry; $C_{15}H_{24}$) is abundant in the plant leaves [12]. The present study has a dual purpose; first to further establish the effectiveness of plant extracts as corrosion inhibitors and second to attempt deduction of the inhibition mechanism and possible adsorption modes of the extract's active components.

2. Experimental

2.1. Materials preparation

Tests were performed on carbon steel specimens with weight percentage composition as follows: C, 0.05; Mn, 0.6; P, 0.36; Si, 0.3; and the balance Fe. The blank corrodents were respectively 1.0 M HCl and 0.5 M H_2SO_4 solutions. Stock solutions of the plant extract were prepared by boiling weighed amounts of the dried and ground leaves of DE under reflux for 3 h in 1.0 M HCl and 0.5 M H_2SO_4 solutions, respectively. The resulting solutions were cooled and then triple-filtered. The amount of plant material extracted into solution was quantified by comparing the weight of the dried residue with the initial weight of the dried plant material before extraction. The resulting filtrates (stock solutions) in both

* Corresponding author.
E-mail addresses: oguziemeka@yahoo.com, emekaoguzie@gmail.com (E.E. Oguzie).

0021-9797/$ - see front matter © 2010 Elsevier Inc. All rights reserved.
doi:10.1016/j.jcis.2010.05.027

cases had a reddish color. From the respective stock solutions, inhibitor test solutions were prepared in the concentration range 5–1000 mg/L in respective corrodents. The effect of iodide ions on inhibition efficiency was studied by combining 5.0 mM KI with low enough concentrations of the extracts to better reflect any enhancements in inhibition performance.

2.2. Gravimetric experiments

Gravimetric experiments were conducted on test coupons of dimension 3 × 3 × 0.14 cm. These were prepared and cleaned as described elsewhere [13]. The precleaned and weighed coupons were suspended in beakers containing the test solutions using glass hooks and rods. Tests were conducted under total immersion conditions in 300 mL of the aerated and unstirred test solutions. To determine weight loss with respect to time, the coupons were retrieved from test solutions at 3-h intervals, appropriately cleaned, dried, and reweighed. The weight loss was taken to be the difference between the weight of the coupons at a given time and its initial weight. All tests were run in triplicate and the data showed good reproducibility. Average values for each experiment were obtained and used in subsequent calculations.

2.3. Electrochemical measurements

Metal samples for electrochemical experiments were machined into cylindrical specimens and fixed in polytetrafluoroethylene (PTFE) rods by epoxy resin in such a way that only one circular surface of area 0.64 cm^2 was left uncovered. The round surface was necessary in order to avoid edge effects. The exposed surface was ground with silicon carbide abrasive paper (from grade #200 to #1000), degreased in acetone, rinsed with distilled water and dried in warm air. Electrochemical experiments were conducted in a Model K0047 corrosion cell using a VERSASTAT 400 complete DC voltammetry and corrosion system, with V3 Studio software. Two graphite rods were used as a counter electrode and a saturated calomel electrode (SCE) as a reference electrode. The latter was connected via a Luggin capillary. Measurements were performed in aerated and unstirred solutions at the end of 1 h of immersion at 303 K. Impedance measurements were made at corrosion potentials (E_{corr}) over a frequency range of 100 kHz–10 mHz, with a signal amplitude perturbation of 5 mV. Potentiodynamic polarization studies were carried out in the potential range ±250 mV versus corrosion potential (in 1 M HCl, which did not show any evidence of passivation) and from −700 to 1600 mV (in 0.5 M H_2SO_4). The scan rate in either case was 0.333 mV s^{-1}. Each test was run in triplicate to verify the reproducibility of the systems.

3. Results and discussion

3.1. Corrosion rates and efficiency of inhibition

We have employed gravimetric and electrochemical techniques to investigate carbon steel corrosion in sulfuric and hydrochloric acid solutions in the absence and presence of DE extract, which is studied herein for corrosion-inhibiting efficacy. The data presented are means of triplicate determinations, with standard deviation ranging from 0 to 0.00071. Fig. 1 shows the weight losses of carbon steel coupons in 1 M HCl and 0.5 M H_2SO_4 without and with different concentrations of DE. The fact that the metal specimen manifests higher corrosion susceptibility in 0.5 M H_2SO_4 is evidence that the acid anions influence the corrosion process in different ways. Fig. 1 also clearly reveals a corrosion-inhibiting effect of DE on both corrodents, which becomes more pronounced with

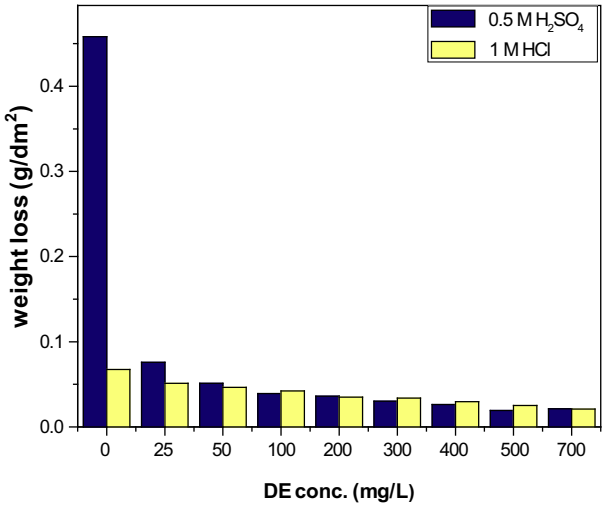

Fig. 1. Weight loss of carbon steel in 1 M HCl and 0.5 M H_2SO_4 without and with different concentrations of DE.

increasing DE concentration, implying a dependence of the inhibition process on the amount of the inhibiting species present in the system. The plots also suggest that DE exerted a greater inhibiting effect in 0.5 M H_2SO_4 than in 1 M HCl.

The corrosion-inhibiting effect of DE can be attributed to phytochemical constituents including alkaloids, carboxylic acids, ketones and alcohols, and ascorbic acid. The different constituents may react with freshly generated Fe^{2+} ions on a corroding metal surface forming organometallic [Fe–Inh] complexes. The inhibiting effect of such complexes then depends on their stability and solubility in the aqueous corrodent, which from our results is a function of the extract concentration and nature of the corrodent.

Quantitative characterization of the inhibiting effect of DE on carbon steel corrosion was achieved from assessment of the inhibition efficiency ($\eta\%$) [13]:

$$\eta\% = \left(1 - \frac{\Delta W_{inh}}{\Delta W_{blank}}\right) \times 100 \quad (1)$$

where ΔW_{inh} and ΔW_{blank} represent the weight losses in inhibited and uninhibited solutions, respectively. Fig. 2 illustrates the variation of inhibition efficiency with DE concentration in 0.5 M H_2SO_4

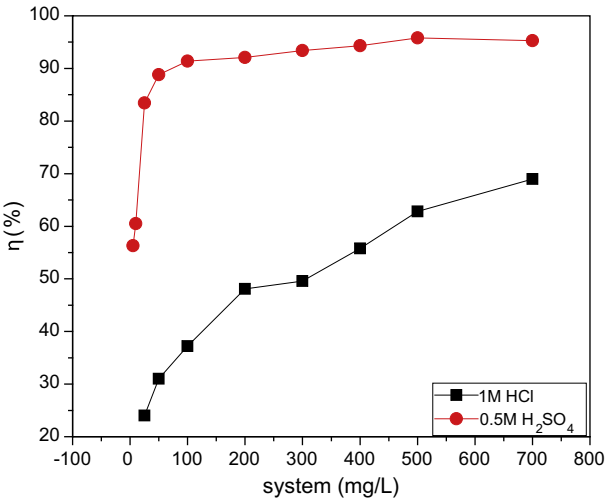

Fig. 2. Variation of $\eta\%$ with different concentrations of DE in 1 M HCl and 0.5 M H_2SO_4.

and 1 M HCl. The plots show that η% increased progressively with inhibitor concentration. It is also obvious that the additive was more effective in 0.5 M H_2SO_4 at all concentrations and attained maximum efficiency more rapidly.

Measurements were also undertaken to understudy the inhibiting effect of DE (at low and high concentrations) from an electrochemical perspective, since the corrosion reaction is essentially an electrochemical process. DE concentrations of 200 mg/L and 800 mg/L were chosen to reflect the features of the inhibiting effect at low and high concentrations, respectively. The evolution of the open circuit potential (E_{OCP}) with time for carbon steel in 1 M HCl and 0.5 M H_2SO_4 solutions without and with DE (200 mg/L and 800 mg/L) is illustrated in Fig. 3. The plots show clear modifications in the E_{OCP}–time behavior due to the presence of DE. In 0.5 M H_2SO_4, an anodic displacement of E_{OCP} is observed on introduction of DE. It is, however, noteworthy that the potential shift in the anodic (noble) direction is more pronounced at low DE concentration. The E_{OCP}–time profiles in 1 M HCl show distinct disparities in the trends at low and high DE concentrations. In the former case (200 mg/L) the attained potential values were always more negative (cathodic) than the values in uninhibited acid, whereas in the latter case (800 mg/L) the E_{OCP} values were more positive. This possibly points toward variations in the inhibition mechanism at low and high DE concentrations in this medium.

Potentiodynamic polarization experiments were undertaken to distinguish the effect of DE on the anodic and cathodic corrosion reactions. The polarization curves for the carbon steel sample in 1 M HCl without and with DE (Fig. 4a) all exhibit active dissolution without any distinctive transition to passivation.

DE is seen to shift E_{corr} in the cathodic direction and the cathodic polarization is also more pronounced than the anodic polarization, indicating that the corrosion process was predominantly under cathodic control [14]. This result was observed at both low and high DE concentrations. The effect of DE on the anodic dissolution process is noticeably dependent on the amount of DE present in the solution. DE is observed to exert a slight depolarizing action on the anodic process at potentials more negative than E_{corr} in the blank acid. This effect persisted for a wider potential range at low DE concentration. High concentrations of DE abridged the depolarization region and even seemed to exert a slight inhibiting effect on the anodic dissolution reaction.

The potentiodynamic polarization behavior of the carbon steel specimen in 0.5 M H_2SO_4 (Fig. 4b) shows distinct features of active–passive transition. It appears that the carbon steel specimen, initially passivated to some extent, then rapidly undergoes pitting corrosion in 0.5 M H_2SO_4. Addition of DE at low concentration promotes passivation, increases the stability of the passive film, and improves resistance to pitting corrosion. At high DE concentra-

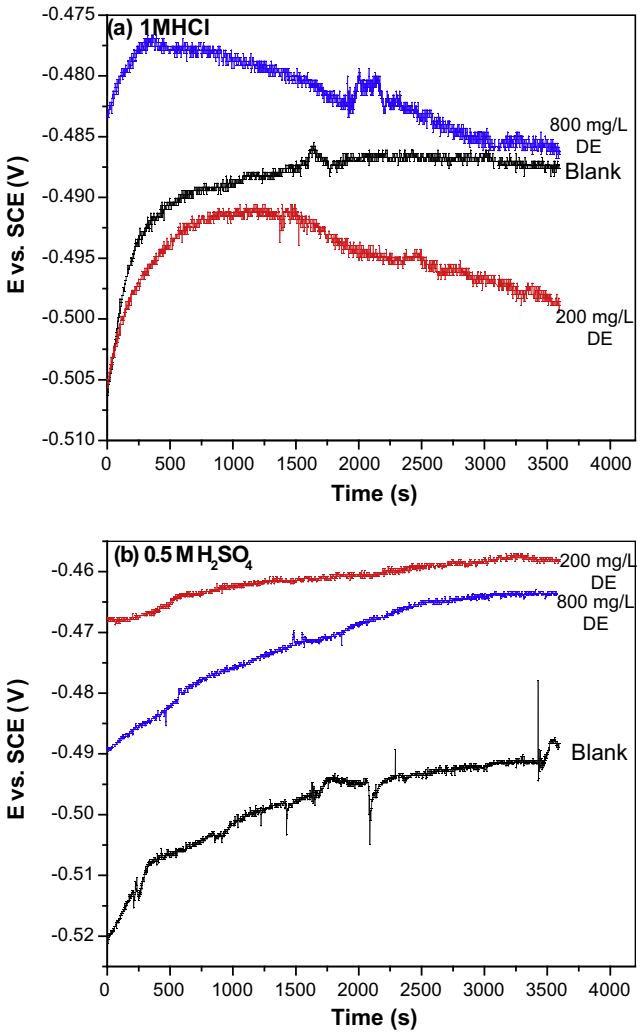

Fig. 3. Open-circuit potential – time variation of carbon steel in: (a) 1 M HCl and (b) 0.5 M H_2SO_4 solution without and with DE.

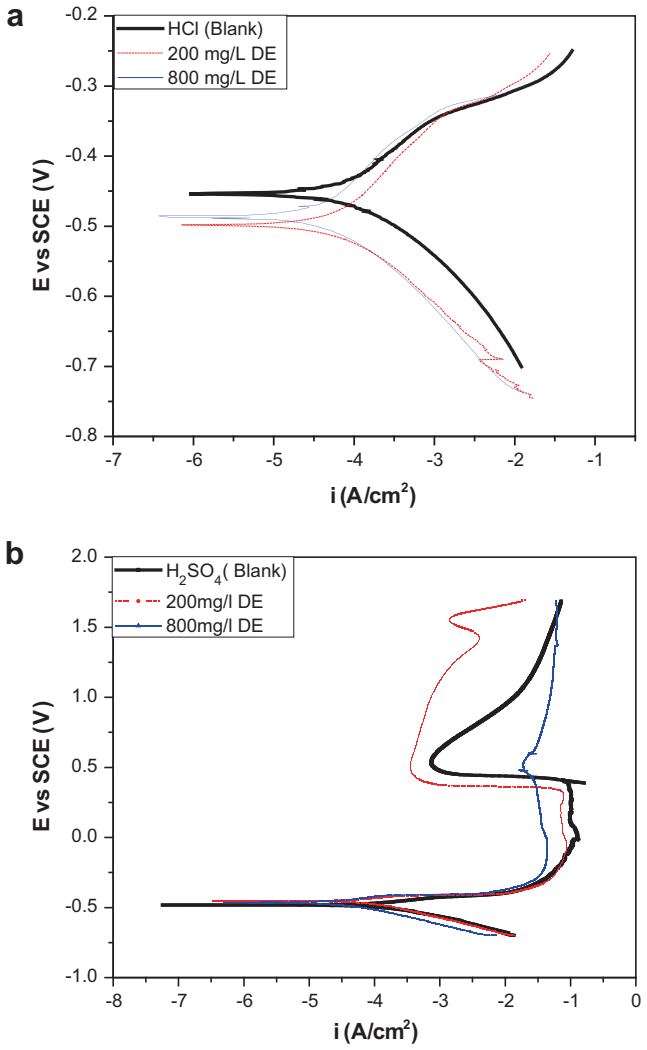

Fig. 4. Potentiodynamic polarization curves of carbon steel in: (a) 1 M HCl and (b) 0.5 M H_2SO_4 solution without and with DE.

tions, on the other hand, the metal shows no tendency toward passivation after the critical current has been attained; rather, the anodic current remains almost steady at this critical value. We attribute this effect at high DE concentrations to the presence of ascorbic acid (AA) in extract. It has been shown that ascorbic acid at sufficiently high concentrations can form $[Fe–AA]^{2+}$ chelates with freshly generated Fe^{2+} ions on a corroding steel surface in sulfuric acid [15]. Such formation of $[Fe–AA]^{2+}$ chelates has also been observed for mild steel corrosion in 0.3% NaCl [16] and brackish water [17] and in the present case leads to a general improvement in inhibition efficiency as well as resistance to pitting corrosion.

Impedance experiments were undertaken to afford insight into the characteristics and kinetics of electrochemical processes occurring at the Fe/1 M HCl and Fe/0.5 M H_2SO_4 interfaces in the absence and presence of DE. The impedance responses of these systems are given in Figs. 5 and 6 in Nyquist and Bode formats respectively. The Nyquist plots generally comprise only one depressed capacitive semicircle in the high-frequency region, which corresponds to one time constant in the Bode plots. The Bode phase angle vs frequency plots comprise peaks at intermediate to high frequencies, which represent the capacitive characters. The observed depression of the Nyquist semicircle with center under the real axis is typical for solid metal electrodes that show frequency dispersion of the impedance data [18,19]. The transfer function can be represented by a solution resistance R_s, shorted by a capacitor C that is placed in parallel to the charge transfer resistance R_{ct} [20]:

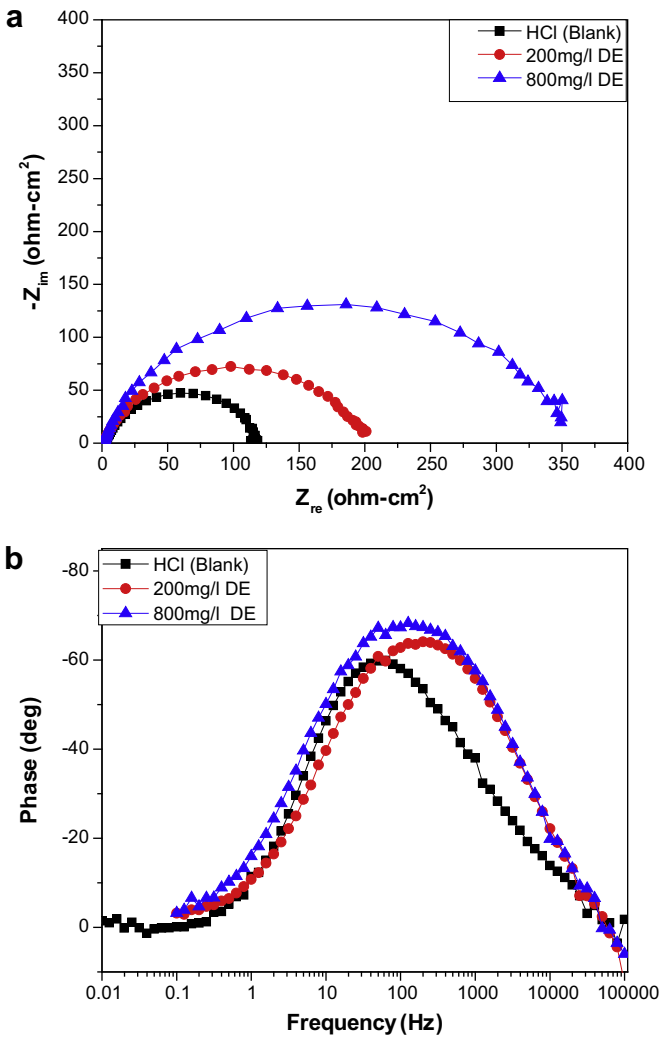

Fig. 5. Electrochemical impedance spectra of carbon steel in 1 M HCl solution without and with DE: (a) Nyquist and (b) Bode phase angle plots.

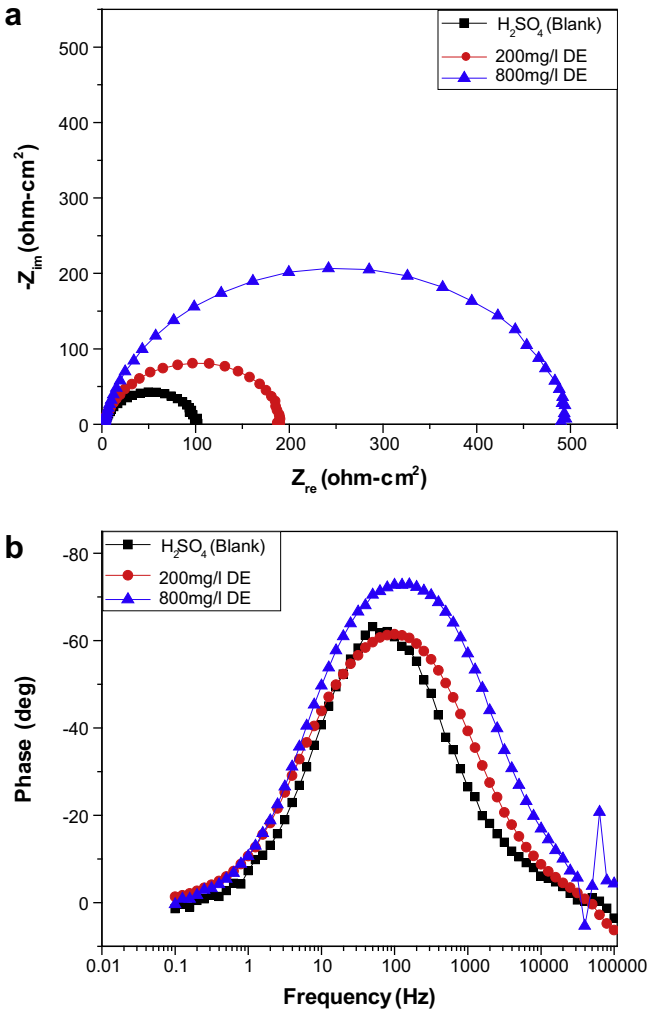

Fig. 6. Electrochemical impedance spectra of carbon steel in 0.5 M H_2SO_4 solution without and with DE: (a) Nyquist and (b) Bode phase angle plots.

$$Z_{(\omega)} = R_s + \left(\frac{1}{R_{ct}} + j\omega C\right)^{-1}. \quad (2)$$

This transfer function is applicable, however, only for homogeneous systems with one time constant when the center of the semicircle lies on the abscissa and cannot account for the depression of the capacitive semicircle. When a nonideal frequency response is present the capacitor is replaced by a constant phase element (CPE). The use of such a CPE accounts for the deviations from ideal dielectric behavior and is related to surface inhomogeneities. The impedance, Z, of the CPE is [19,20]:

$$Z_{CPE} = Q^{-1}(j\omega)^{-n}, \quad (3)$$

where Q and n stand for the CPE constant and exponent, respectively, $j = (-1)^{1/2}$ is an imaginary number, and ω is the angular frequency in rad s^{-1} ($\omega = 2\pi f$ when f is the frequency in Hz). The impedance spectra for the Nyquist plots were appropriately analyzed by fitting to the equivalent circuit model $R_s(Q_{dl}R_{ct})$, which has previously been used to model the Fe/acid interface [21]. The corresponding electrochemical parameters given in Table 1 reveal that introduction of DE into the acid corrodents caused the charge transfer resistance to increase, while reducing the double-layer

Table 1
Electrochemical impedance parameters for carbon steel in 1 M HCl and 0.5 M H_2SO_4 in the absence and presence of DE.

System	R_{ct} (Ω cm^2)	Q_{dl} ($\mu\Omega^{-1}$ s^n cm^{-2})	N	η%
1 M HCl				
Blank	119.7	504	0.79	–
200 mg/L DE	197.5	220	0.81	39.4
800 mg/L DE	351.5	189	0.82	66.0
0.5 M H_2SO_4				
Blank	103.9	461	0.81	–
200 mg/L DE	181.1	267	0.82	42.6
800 mg/L DE	497.2	79.9	0.89	79.1

capacitance. This effect becomes more pronounced at higher DE concentration. This increase in the diameter of the Nyquist semicircle (R_{ct} values), including the corresponding increase in the magnitude of the phase angle peaks in inhibited solutions, points toward improved corrosion resistance due to the corrosion-inhibiting action of DE. The decrease in C_{dl} values, which normally results from a decrease in the dielectric constant and/or an increase in the double-layer thickness, can be attributed to the adsorption of DE onto the metal/electrolyte interface. This implies that DE reduces the corrosion rate of the mild steel specimen in both 0.5 M H_2SO_4 and 1 M HCl by adsorption of the extract organic matter onto the metal surface immersed in the acid media, thereby protecting the metal from corrodent attack. The parameter n is generally accepted to be a measure of surface inhomogeneity, and its increase in the inhibited solution compared to the pure acid is connected with a decrease in heterogeneity resulting from inhibitor adsorption.

Efficiency of inhibition is observed from Table 1 to increase with DE concentration. The values were estimated by comparing the values of the charge transfer resistance in the absence ($R_{ct,bl}$) and presence of inhibitor ($R_{ct,inh}$) as follows [18,20]:

$$\eta\% = \left(1 - \frac{R_{ct,inh} - R_{ct,bl}}{R_{ct,inh}}\right)100 \quad (4)$$

The values differ somewhat from those obtained from gravimetric measurements due basically to factors associated with the different techniques, but the trend remains the same.

3.2. Adsorption considerations

The complex nature of the corrosion inhibition process is not in doubt. This complexity is increased by several orders of magnitude when one considers plant extracts with their complicated chemical compositions. This makes it difficult to assign the inhibitive effect to adsorption of any particular constituent, since some of these constituents, including tannins, organic and amino acids, alkaloids, proteins, flavonoids, and organic pigments and their acid hydrolysis products, are known to exhibit inhibiting action [22–25]. Zucchi and Omar [22] attributed the inhibiting effect of acid extracts of some plant materials to protonated species resulting from protein hydrolysis products, and although we are as yet unable to ascertain the actual species responsible for the corrosion-inhibiting efficacy of DE, certain experimentally determined features can offer a general overview.

In the acid extracts used in this study, the majority of the organic constituents should exist as protonated species and others in the molecular form. The protonated species can be adsorbed onto cathodic sites on the corroding metal surface and reduce H_2 gas evolution, whereas the molecular species could be chemisorbed at active anodic sites and restrict the anodic dissolution reaction. According to Hackerman and Makrides [26], chemisorbed species may also cause inhibition by increasing the activation overpotential for hydrogen discharge, i.e., poisoning the cathode. The predominant effect will depend on the specific conditions of the process, including the type of acid anion. Again, the mixed-inhibition mechanism suggested by the polarization data provides evidence of adsorption of protonated and molecular species from the DE extract in 1 M HCl and 0.5 M H_2SO_4. Since a corroding steel specimen carries a positive surface charge in both sulfuric and hydrochloric acid solutions, protonated species should be poorly adsorbed. Then again, the ability of chloride ions to be specifically adsorbed onto the positively charged metal surface, thereby reversing the sign of the surface charge and hence facilitating adsorption of protonated inhibitor species, is an important consideration. So a comparison of the inhibition efficiency of the extract in 1 M HCl and 0.5 M H_2SO_4 should reveal the principal modes of adsorption of the extract species. If corrosion inhibition is due exclusively to protonated species that adsorb electrostatically, the extract should be more effective in 1 M HCl; if not, then the inhibiting effect should be comparable in both acid solutions or even more pronounced in 0.5 M H_2SO_4 [27].

Another consideration involved an assessment of the influence of halide additives on inhibitor adsorption. It is generally accepted that introduction of halide ions facilitates adsorption of organic-cation-type inhibitors during mild steel corrosion in acidic solution. This ability increases in the order $Cl^- < Br^- < I^-$ [28,29] and is also initiated by the specific adsorption of the anion onto the metal surface, as mentioned earlier. Again, if the protonated species contribute significantly to the inhibiting effect of the extract, a synergistic increase in inhibition efficiency should be observed in the presence of the halide additives. On the other hand, if molecular species in the extract are more active, the halide additives will have negligible effect. The comparatively higher η% values in 0.5 M H_2SO_4 at all studied concentrations perhaps imply that the nonprotonated constituents make the predominant contribution. On the other hand, Fig. 7 clearly shows that iodide ions remarkably enhanced the inhibition efficiency of the extract in both acid solutions, thus confirming an important role of the protonated species, which is enhanced in the presence of the iodide ions thereby resulting in improved surface coverage and inhibition efficiency.

Assuming a direct relationship between inhibition efficiency and the degree of surface coverage (θ) [$\eta\% = 100 \times \theta$] for different inhibitor concentrations, data obtained from gravimetric measurements were adapted to determine the adsorption characteristics of DE on mild steel in the different acid media according to the Langmuir equation [30]:

$$C/\theta = 1/b + C. \quad (5)$$

The plot of C/θ vs. C is shown in Fig. 8 to be linear for DE in both 1 M HCl and 0.5 M H_2SO_4 (with slopes of 1.35 and 1.04, respectively), suggesting that the experimental data follow the Langmuir isotherm. The divergence of the slope from unity and the nonzero intercepts on the y-axes, which is more pronounced for 0.5 M HCl, is attributable to interactions between adsorbate species on the metal surface as well as changes in the adsorption heat with increasing surface coverage. This also implies that the extract active species occupy more than one active site on the metal surface. More importantly, however, a close inspection of the Langmuir isotherm plot for DE in 1 M HCl reveals two distinct linear regions at low and high concentrations. We highlighted these linear regions with their corresponding slopes and labeled them A and B, respectively. If we assume that unit slopes correspond to a tendency toward monolayer adsorption, then the wide variation in the slopes from low to high concentrations could mean that two different mechanisms are in operation, which is akin to transformation from multilayer (physisorption) (slope = 1.76) to monolayer (chemi-

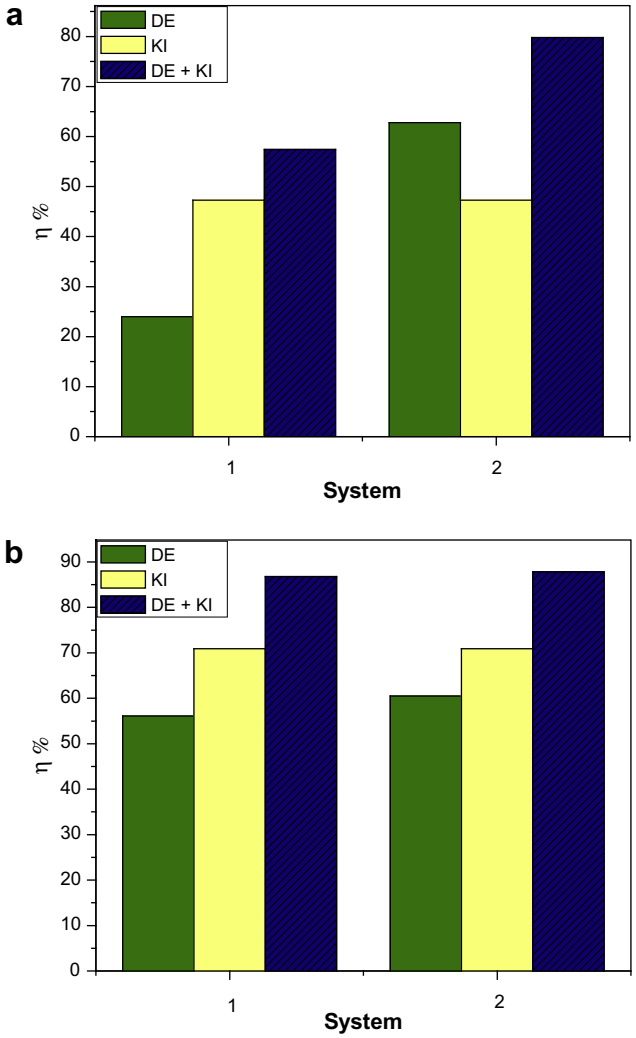

Fig. 7. Inhibition efficiencies of DE, 0.5 mM KI, and DE + KI in: (a) 1 M HCl (1 = 25 mg/L DE, 2 = 500 mg/L DE) and (b) 0.5 M H_2SO_4 (1 = 5 mg/L DE, 2 = 10 mg/L DE).

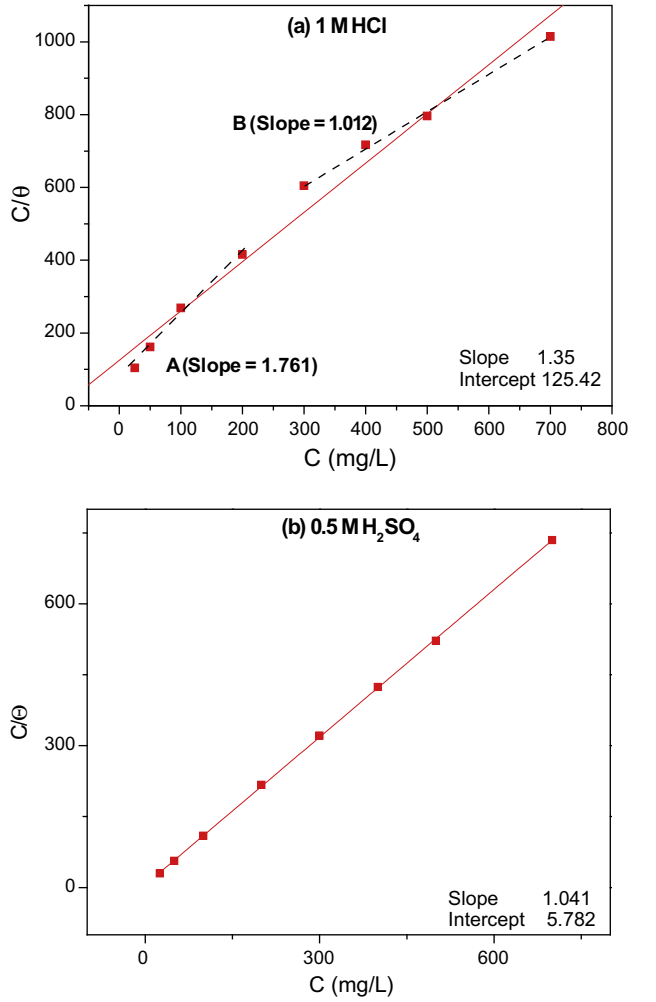

Fig. 8. Langmuir adsorption isotherm for DE on carbon steel in: (a) 1 M HCl and (b) 0.5 M H_2SO_4 solution.

sorption) at high concentrations (slope = 1.01) when some extract constituents are present in sufficient amounts to react with the metal surface and even form chelates as suggested for ascorbic acid.

Our experimental results show that the corrosion-inhibiting efficacy of DE extract results from adsorption of the extract organic matter on the corroding metal surface. This normally results from Lewis acid–base interactions in which the metal and inhibitor molecules act as a Lewis acid and Lewis base, respectively, and their interaction is accomplished by favorable overlap of frontier orbitals and sharing of electrons between the inhibitor and the partially filled *d*-orbitals of the metal [31,32]. A practical route to studying the complex processes associated with metal–inhibitor interactions at the molecular level involves computer simulations of suitable models, and density functional theory (DFT) has been used widely in this regard [31–35]. An approach we are currently investigating for plant extracts with their intricate chemical composition involves qualitative characterization of the phytochemical constituents coupled with elucidation of their molecular structures. We then model the molecular structures using a combination of DFT-based quantum-chemical calculations and molecular dynamics simulations to theoretically evaluate the inhibiting potential based on structure–activity relationships to estimate basic molecular descriptors such as molecular surface area, frontier molecular orbitals, charge densities, and ionization potential, which contribute to the corrosion-inhibiting effect. We have performed such calculations to model the adsorption structures of the major chemical constituents of DE extract (caryophyllene [Cry], ascorbic acid [AA], and the alkaloid [HBMB]) and hence provide some insight into the nature of their interaction with the mild steel surface and their possible contributions to the overall inhibiting effect. The calculations were performed by means of the DFT electronic structure program $DMol^3$ using a Mulliken population analysis [36,37]. Electronic parameters for the simulation include restricted spin polarization using the DND basis set and the Perdew–Wang (PW) local-correlation-density functional. The molecular structures were first subjected to geometry optimization using a COMPASS force field and the Smart minimization method by high-convergence criteria. We then determined the electronic structures of molecules, including the distribution of frontier molecular orbitals and Fukui indices, in order to establish the active sites as well as the local reactivity of the molecules. The optimized structures, the highest occupied molecular orbital (HOMO), and the lowest unoccupied molecular orbital (LUMO), as well as the total electron density of Cry, AA, and HBMB, are presented in Fig. 9.

The regions of highest electron density (HOMO) are the sites at which electrophiles attack and represent the active centers, with the utmost ability to bond to the metal surface, whereas the LUMO

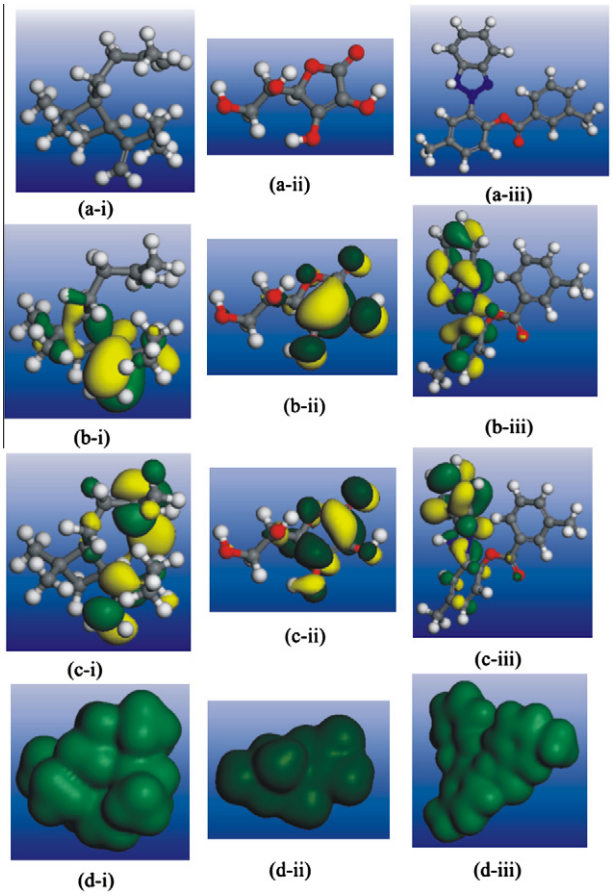

Fig. 9. Electronic properties of (i) Cry; (ii) AA; (iii) HBMB: (a) optimized structure, (b) HOMO orbital, (c) LUMO orbital, (d) total electron density. (Atom legend: white = H; gray = C; red = O; blue = N.) (For interpretation of the references to colour in this figure legend, the reader is referred to the web version of this article.)

orbital can accept the electrons in the *d*-orbital of the metal (Fe) using antibonding orbitals to form feedback bonds [31]. We observe that the HOMO orbital for Cry is saturated around the C=C double bond while that of AA is mainly around the lactone nucleus. The electron density (charge distribution) is saturated all around each molecule; hence we should expect flat-lying adsorption orientations. The local reactivity of the molecules was analyzed by means of the Fukui indices (FI) to assess reactive regions in terms of nucleophilic (f^+) and electrophilic attack (f^-). We observed that the f^- functions of all the molecules (not shown) correspond with the HOMO locations, indicating the zones through which the molecule will be adsorbed onto the Fe surface.

Table 2 provides some quantum-chemical parameters related to the molecular electronic structure of the most stable conformation of the molecules. High values of E_{HOMO} indicate the disposition of the molecule to donate electrons to an appropriate acceptor with vacant molecular orbitals. In the same way, low values of the energy of the gap $\Delta E = E_{LUMO-HOMO}$ will render good inhibition efficiencies since the energy to remove an electron from the last occupied orbital will be minimized. The dipole moment is the first derivative of the energy with respect to an applied electric field and is a measure of the asymmetry in the molecular charge distribution. A low value of the dipole moment favors accumulation of inhibitor molecules on the metal surface and is also an indication of the hydrophobic character of the molecule. Values of μ ranging from 3 to 5 have been reported in the literature [32–35].

Our obtained values do not show any well-defined correlations, and none was actually expected, since the molecules differ considerably in their chemical structures and we do not yet know their individual inhibition efficiencies. Nonetheless, certain features point toward the individual corrosion-inhibiting efficacies of the molecules. For instance, the calculations indicate that the AA molecule has the highest HOMO energy (−6.081 eV), indicating a stronger tendency of the molecule to donate electrons to appropriate acceptor molecules of low empty molecular orbital energy. Cry has the lowest E_{LUMO} value, showing that the molecule would readily accept electrons from the metal d-orbital. HBMB on the other hand has the lowest ΔE value, which corresponds to higher stability of the [Fe–HBMB] complex as well as high values of the dipole moment and polarizability, which describe the reactivity of the inhibitor molecule toward the metal surface [36].

We also performed molecular dynamics (MD) simulations to illustrate the adsorption of the molecules onto the corroding metal surface at a molecular level. This was achieved using Forcite quench molecular dynamics in the MS Modeling 4.0 software to sample many different low-energy configurations and identify the low energy minima [38,39]. Calculations were carried out in

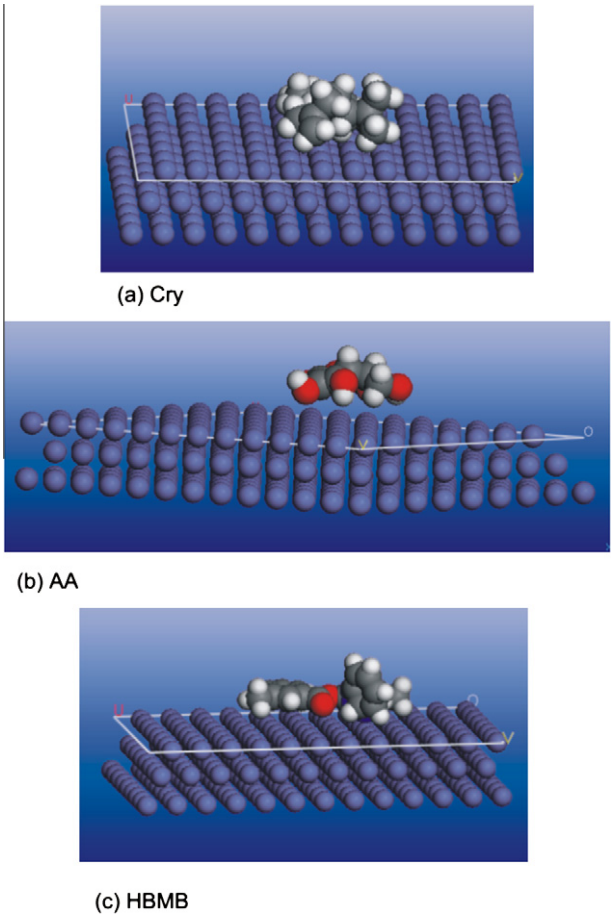

Fig. 10. Molecular dynamics model of the adsorption of single molecules of: (a) Cry, (b) AA, and (c) HBMB on Fe (1 1 0) surface.

Table 2
Calculated quantum-chemical properties for the most stable conformations of Cry, AA, and HBMB.

Property	Cry	AA	HBMB
E_{HOMO} (eV)	−5.558	−6.081	−4.604
E_{LUMO} (eV)	−0.676	−2.303	−2.681
$E_{LUMO-HOMO}$	4.882	3.778	1.923
μ_{Total} (debye)	0.334	2.188	4.619
Molecular surface area (sq. Å)	293.68	179.90	415.85

a 12 × 8 supercell using the COMPASS force field and the Smart algorithm. The Fe crystal was cleaved along the (1 1 0) plane. Temperature was fixed at 350 K, with NVE (microcanonical) ensemble, with a time step of 1 fs and simulation time 5 ps. The system was quenched every 250 steps. Optimized structures of Cry, AA, HBMB, and the Fe surface were used for the simulation. Using the quench molecular dynamics method above, we found the preferred binding sites for the molecules on the Fe surface and calculated the binding energy. Fig. 10a–c show the optimized (lowest-energy) adsorption models for single molecules of Cry, AA, and HBMB, respectively, on the Fe (1 1 0) surface from our simulation. Solvent and charge effects have been neglected. The molecules can be seen to maintain a flat-lying adsorption orientation on the Fe surface, with the regions of high HOMO density acting as the adsorption sites.

The binding energy (E_{Bind}) between each molecule and the Fe surface was calculated using the following equation [40]:

$$E_{Bind} = E_{total} - (E_{Met} + E_{Fe}). \quad (6)$$

In each case the potential energies were calculated by averaging the energies of the five structures of lowest energy. The obtained values were −119 kcal/mol, −77.2 kcal/mol, and −142.7 kcal/mol for Cry, AA, and HBMB, respectively. Bartley et al. [40] observed a good linear correlation between inhibition efficiency and binding energy, wherein efficiency increased with binding energy. HBMB, with the lowest ΔE value, still has the highest E_{Bind}, implying an important contribution of this compound to the observed inhibiting effect. Interestingly, also, the trend of E_{Bind} means that Cry, which is essentially a hydrocarbon with no heteroatom, is more effective than AA. This, however, is very unlikely considering the proven ability of AA to form chelates with Fe^{2+} ions, as well as the lower ΔE value and higher values of E_{HOMO} and μ. What this implies is that it is misleading to attempt to theoretically ascertain corrosion-inhibiting potential from a single parameter. Again the anticipated situation at high DE concentrations cannot be obvious from modeling adsorption of a single molecule onto the Fe surface, without considering the interactions between adjacent molecules. But then, the situation where many molecules occupy the surface is much more complex and more difficult to model and is still being investigated.

It is clear from our theoretical studies that the corrosion-inhibiting properties of the different extract constituents do not follow any well-defined or regular trend and any one of them could exert a dominant effect under specific conditions and concentrations. In other words, as the extract concentration is varied, certain features could become enhanced or suppressed leading to the observed difference in inhibition mechanisms at low and high DE concentrations.

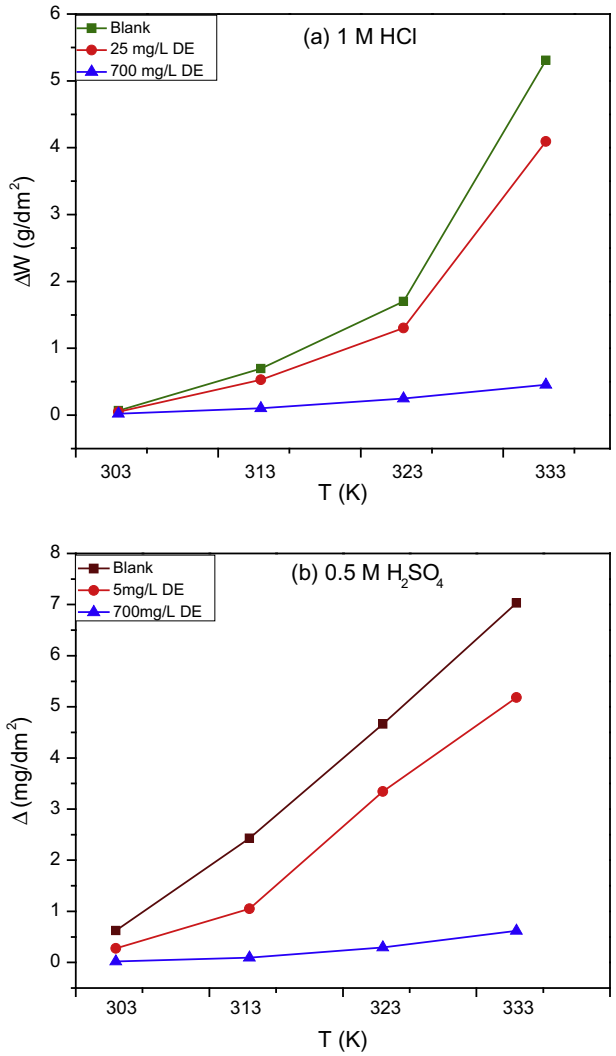

Fig. 11. Effect of temperature on the corrosion rates of carbon steel in: (a) 1 M HCl and (b) 0.5 M H_2SO_4 without and with DE.

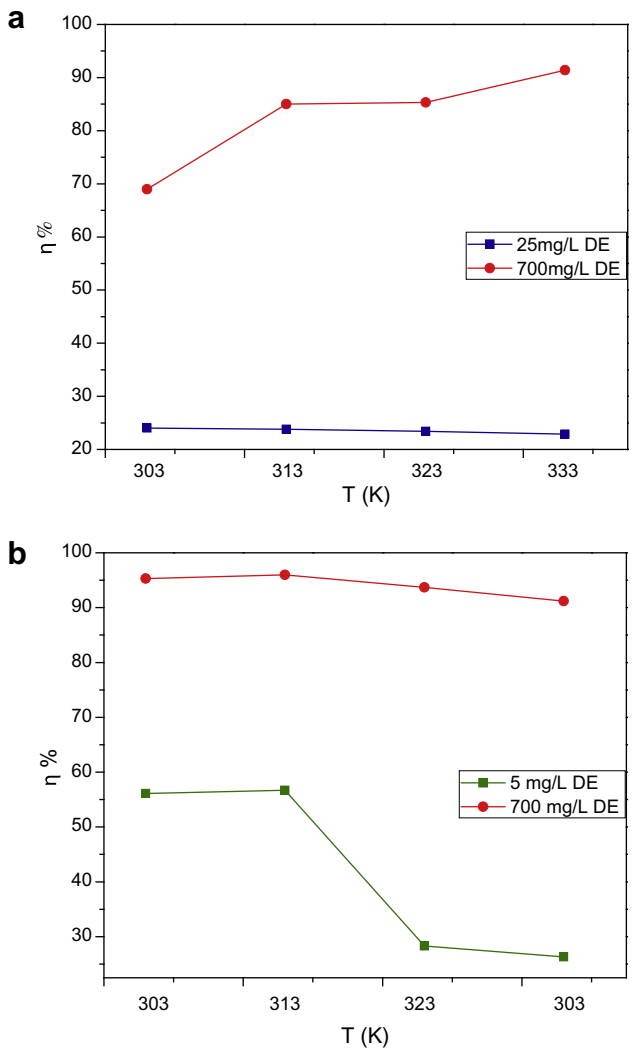

Fig. 12. Effect of temperature on the inhibition efficiency (η%) of DE for carbon steel corrosion in: (a) 1 M HCl and (b) 0.5 M H_2SO_4.

3.3. Effect of temperature

When the electrochemical corrosion reaction involves a cathodic process of hydrogen depolarization, the corrosion rate increases exponentially with rise in temperature, according to Arrhenius-type dependence. We therefore assessed the effect of temperature variation on the corrosion and corrosion inhibition processes by conducting gravimetric tests at 303–333 K in both uninhibited and inhibited systems (1 M HCl; HCl + 25 mg/L DE; HCl + 700 mg/L DE) and (0.5 M H_2SO_4; H_2SO_4 + 25 mg/L DE; H_2SO_4 + 700 mg/L DE). DE concentrations were selected to properly reflect the temperature effects at low and high surface coverage. The results obtained after a 3-h immersion period are presented in Fig. 11 and show that corrosion rates in both uninhibited and inhibited acids increased with rise in temperature. Also, DE is seen to maintain its inhibiting effect at all temperatures.

Fig. 12 illustrates the trend of inhibition efficiency with temperature. In 0.5 M H_2SO_4, we observe a reduction in inhibition efficiency with rise in temperature at low DE concentration. This could be attributed to the shift of the adsorption–desorption equilibrium toward desorption. Similar behavior is also seen at low DE concentrations in 1 M HCl, while efficiency increased with temperature at high DE concentration.

The Arrhenius-type relationship between the corrosion rate (k) of mild steel in acidic media and temperature (T) as often expressed by the Arrhenius equation was used to determine the activation energies (E_a):

$$k = A\exp(-E_a/RT). \quad (7)$$

A is the preexponential factor and R the universal gas constant. The variation of logarithm of corrosion rate with reciprocal of absolute temperature is shown in Fig. 13 for 0.5 M H_2SO_4 and 1 M HCl without and with DE. The calculated values of E_a are given in Table 3. Addition of DE is seen to increase E_a for the corrosion reaction in 0.5 M H_2SO_4 at low and high concentrations, while a high concentration of DE reduced the activation energy in 1 M HCl.

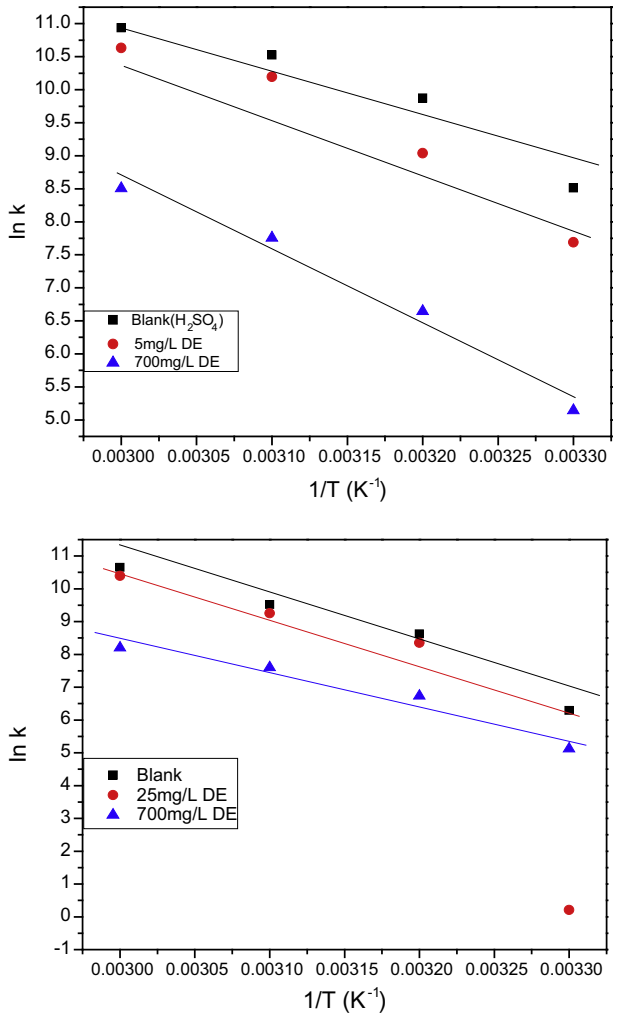

Fig. 13. Arrhenius plots for carbon steel corrosion in: (a) 1 M HCl and (b) 0.5 M H_2SO_4 without and with DE.

Table 3
Activation parameters for carbon steel corrosion in 1 M HCl and 0.5 M H_2SO_4 without and with DE.

System	E_a (kJ mol^{-1})	Q_{ads} (kJ mol^{-1})
1 M HCl		
Blank	116.32	–
25 ppm	116.73	−1.71
700 ppm	84.03	39.19
0.5 M H_2SO_4		
Blank	65.89	–
5 ppm	82.98	−41.73
700 ppm	93.09	−20.72

The decrease in η% of DE with rise in temperature observed in 0.5 M H_2SO_4, including the higher E_a values in the presence of DE, is often assumed to be indicative of physical adsorption of inhibitor species onto a corroding metal surface [41,42]. A similar trend is also seen in 1 M HCl at low DE concentration. The opposite effect, observed at high DE concentration in 1 M HCl, i.e., an increase in η% with increasing temperature, indicates inhibitor chemisorption. As suggested earlier, at sufficiently high DE concentrations some of the constituents, including ascorbic acid, undergo chemical reaction and even chelate the surface Fe atoms. The reaction rate increases with rising temperature as with other chemical reactions, yielding improved surface coverage, and hence improved inhibition efficiency. This behavior further confirms our earlier deductions from the features of the Langmuir isotherm of DE from 0.5 M HCl.

4. Conclusions

DE extract functioned as an inhibitor of carbon steel corrosion in 1 M HCl and 0.5 M H_2SO_4 solutions. Polarization measurements suggest a mixed-inhibition mechanism, which the impedance data indicate was achieved via adsorption of the extract species on the carbon steel surface. The adsorption behavior, as approximated by the Langmuir isotherm, shows distinct discrepancies going from low to high DE concentration in 1 M HCl, which we have correlated with a transformation from physisorption at low concentrations to chemisorption at sufficiently high concentrations. This agrees well with the trend of inhibition efficiency with temperature as well as values of activation energy. DFT-based quantum-chemical computations of parameters associated with the electronic structures of specific components of the extract confirmed their inhibiting potential, which was further corroborated by molecular dynamic modeling of the adsorption of the single molecules onto the metal surface.

Acknowledgments

This project is funded by TWAS, the Academy of Sciences for the Developing World, under the TWAS Grants for Research Units in Developing Countries Program (TWAS-RGA08-005). We also acknowledge financial support from the Vice Chancellor and the

Senate Research Grants Committee of the Federal University of Technology Owerri.

References

[1] G. Gunasekaran, L.R. Chauhan, Electrochim. Acta 49 (2004) 4387.
[2] A.Y. El-Etre, Corros. Sci. 45 (2003) 2485.
[3] M. Abdallah, Corros. Sci. 46 (2004) 1981.
[4] Y. Li, P. Zhao, Q. Liaqng, B. Hou, Appl. Surf. Sci. 252 (2005) 1245.
[5] A.Y. El-Etre, M. Abdallah, Z.E. El-Tantawy, Corros. Sci. 47 (2005) 385.
[6] L.R. Chauhan, G. Gunasekaran, Corros. Sci. 49 (2007) 1143.
[7] P.B. Raja, M. Sethuraman, Mater. Lett. 62 (2008) 2922.
[8] E.E. Oguzie, Corros. Sci. 50 (2008) 2993.
[9] P.C. Okafor, M.E. Ikpi, I.E. Uwah, E.E. Ebenso, U.J. Ekpe, S.A. Umoren, Corros. Sci. 50 (2008) 2310.
[10] A.M. Abdel-Gaber, B.A. Abd-El-Naber, I.M. Sidahmed, A.M. El-Zayady, M. Saadawy, Corros. Sci. 48 (2006) 2765.
[11] D.E. Okwu, B.U. Ighodaro, Int. J. Drug Dev. Res. 1 (2009) 117.
[12] L.C. Obame, P. Edou, H.N. Bassole, J. Koudou, A. Agnaniet, F. Eba, A.S. Traore, Afr. J. Microbiol. Res. 2 (2008) 148.
[13] E.E. Oguzie, Mater. Lett. 59 (2005) 1076.
[14] C. Cao, Corros. Sci. 38 (1996) 2073.
[15] E.E. Oguzie, Y. Li, F.H. Wang, J. Appl. Electrochem. 37 (2007) 1183.
[16] I. Sekine, Y. Nakahata, H. Tanabe, Corros. Sci. 28 (1988) 987.
[17] A.N. Nigam, R.P. Tripathi, M.L. Jangid, K. Dhoot, M.P. Chacharkar, Corros. Sci. 30 (1990) 201.
[18] A. Popova, S. Raicheva, E. Sokolova, M. Christov, Langmuir 12 (1996) 2083.
[19] K.F. Khaled, N. Hackerman, Electrochim. Acta 48 (2003) 2715.
[20] G. Moretti, F. Guidi, G. Grion, Corros. Sci. 46 (2004) 387.
[21] G. Mu, X. Li, J. Colloid Interface Sci. 289 (2005) 184.
[22] F. Zucchi, I.H. Omar, Surf. Technol. 24 (1985) 391.
[23] S. Martinez, I. Stern, J. Appl. Electrochem. 31 (2001) 973.
[24] M.A.S. Quraishi, in: Proceedings of the Corrosion 2004, Paper No. 04411, NACE International, Houston, TX, 2004.
[25] M. Kliskic, J. Radosevic, S. Gudic, V. Katalinic, J. Appl. Electrochem. 30 (2000) 823.
[26] N. Hackerman, A.C. Makrides, Ind. Eng. Chem. 46 (1954) 523.
[27] A. Popova, E. Sokolova, S. Raicheva, M. Christov, Corros. Sci. 45 (2003) 33.
[28] E.E. Oguzie, Mater. Chem. Phys. 87 (2004) 212.
[29] E.E. Oguzie, G.N. Onuoha, A.I. Onuchukwu, Mater. Chem. Phys. 89 (2004) 305.
[30] M. Lebrini, F. Bentiss, H. Vezin, M. Lagrenee, Corros. Sci. 48 (2006) 1279.
[31] S. Martinez, I. Stagljar, Theochem 640 (2003) 167.
[32] K.F. Khaled, K. Babic-Samardzija, N. Hackerman, Electrochim. Acta 50 (2005) 2515.
[33] J. Cruz, E. Garcıa-Ochoa, M. Castro, J. Electrochem. Soc. 150 (2003) 26.
[34] L. Marıa Rodrıguez-Valdez, W. Villamisar, M. Casales, J.G. Gonzalez-Rodriguez, A. Martınez-Villafane, L. Martinez, D. Glossman-Mitnik, Corros. Sci. 48 (2006) 4053.
[35] J.M. Roque, T. Pandiyan, J. Cruz, E. Garcıa-Ochoa, Corros. Sci. 50 (2008) 614.
[36] B. Delley, J. Chem. Phys. 92 (1990) 508.
[37] B. Delley, J. Chem. Phys. 113 (2000) 7756.
[38] C.J. Casewit, K.S. Colwell, A.K. Rappé, J. Am. Chem. Soc. 114 (1992) 10035.
[39] C.J. Casewit, K.S. Colwell, A.K. Rappé, J. Am. Chem. Soc. 114 (1992) 10046.
[40] J. Bartley, N. Huynh, S.E. Bottle, H. Flitt, T. Notoya, D.P. Schweinsberg, Corros. Sci. 45 (2003) 81.
[41] E.E. Ebenso, Bull. Electrochem. 19 (2003) 209.
[42] G.K. Gomma, Mater. Chem. Phys. 55 (1998) 241.